Trans., Geothermal Resources Council, Vol. 27, 2003

A Simple, Fast Method of Estimating Fractured Reservoir Geometry from Tracer Tests

G. Michael Shook
Idaho National Engineering and Environmental Laboratory

Abstract
A simple method of estimating flow geometry and pore geometry from conservative tracer tests in single phase geothermal reservoirs is shown. The tracer effluent history at any given production well is used in an Excel spreadsheet application to estimate relative flow vs. storage capacity. In a set of simple numerical experiments the flow and storage geometries estimated using this analysis agrees very well with known geometries. Open flow boundaries do not change the accuracy of the method.

Key Words
Tracer tests, fractured reservoirs, flow capacity, storage capacity, F-C diagrams

Introduction
Tracer testing in geothermal fields is a mature practice, with more than 100 tests conducted in the last decade (Adams, personal communication). In the broadest sense, tracer tests are used to determine flow paths in the reservoir; the longer the flow path, the less chance of injection-induced cooling of produced fluids. More specifically, tracer tests can and should be used to determine reservoir swept volume, fluid velocities, and reservoir geometry, and use this information to estimate the onset of cooling at extraction wells.

Current tracer test analysis methods in the geothermal literature are a mixture of qualitative and numerical. Most tracer test analysis is a qualitative determination of the connectivity of injection and production wells (e.g., Rose et al., 2001; Adams, et al., 2001; Gunderson et al., 2002). The time history of the tracer may be collected at some production wells, but that data is not typically used in an analysis. Some bulk reservoir properties have been inferred from the tracer tests. For example, Rose et al. (1996) estimated the pore volume of the Beowawe geothermal reservoir from tracer dilution calculations. From a series of Dixie Valley tracer tests, Rose et al. (2001) noted a directional dependence in tracer recovery, which lead to inference of a barrier to flow between Sections 33 and 7 (Rose, 2002). Gunderson et al. (2002) inferred the presence of permeability anisotropy at Awibengkok by noting that fluid flow (as determined from tracer recovery) occurred at oblique angles to pressure gradients.

Other researchers have attempted to combine tracer test analysis with numerical models, primarily to constrain the conceptual reservoir model. Axelsson et al. (2001) concluded from tracer tests at the Laugaland, Iceland geothermal field that injected water travels through the reservoir by two methods: direct paths (channels) along fractures, and dispersion and mixing through a larger part of the reservoir. On the basis of this conceptual model, an excellent match of tracer recovery curves was obtained. The

conceptual model was subsequently used in estimating future injection-induced cooling. That model is based on one-dimensional channel flow. This is not likely the true reservoir geometry, but is consistent with the conceptual model from tracer flow. In this author's opinion, the Axelsson et al. analysis is the best shown in the geothermal literature to date. Not only was a conceptual model of the flow developed, but attempts at determining flow geometry were also made.

Quantitative geothermal reservoir characterization using tracers has at its roots techniques originally developed for chemical engineering (Levenspiel, 1972). Robinson and Tester (1984) analyzed tracer tests conducted at the Fenton Hill Hot Dry Rock (HDR) reservoir. They defined a modal volume as the reservoir volume corresponding to low impedance fracture connections. This volume can be determined from flow rates and the time at which the tracer effluent concentration is at a maximum. Robinson and Tester (1984) also determine total reservoir pore volume, which is calculated from the mean residence time of the tracer and flow rates. Although it appears that the modal volume should be related to the most likely (in a statistical sense) fracture impedance rather than the low-impedance value, this is nevertheless an effort at extracting reservoir geometry from tracer tests. Similar geometric considerations were applied by Matsunaga et al. (2002) on Hijiori HDR tracer test data. On the basis of changes in modal volumes, the authors concluded that anhydrite scale was plugging some fractures, thereby changing the flow field.

It is recognized that tracer test interpretation in fractured media is difficult. One goal of test interpretation is estimating thermal sweep efficiency in the reservoir. That is, how much energy can be extracted from the rock before the produced fluids experience cooling. There exist a number of variables that impact the sweep efficiency, most notably fracture geometry variables such as flow geometry vs. pore geometry, surface area for heat exchange, and total pore volume between injection/production well pairs. Knowledge of these properties allows the engineer to develop a good conceptual model of the fractured reservoir, which can be used in numerical modeling or other resource management activities.

The Geothermal Program at the Idaho National Engineering and Environmental Laboratory (INEEL) is continuing work on tracer test interpretation methods for fractured reservoirs. This work is an extension of methods previously developed for porous media (Shook, 2001). In particular, we are developing means of estimating reservoir geometry from tracer tests. These results will be used to extend methods of estimating thermal velocities and heat transfer surface areas, and will help constrain numerical reservoir models. This paper summarizes the means of estimating fracture geometry (flow vs. volume) from a conservative tracer test. Work continues on methods for applying this analysis to surface area and thermal velocity estimates.

Flow Capacity – Storage Capacity

The concept of flow vs. storage was developed originally in the petroleum literature to estimate injection sweep efficiency in layered media. The method relates the relative velocity of a given layer to its associated pore volume, usually in a flow-storage diagram.

It can be used semi-quantitatively to describe reservoir geometry (e.g., "40% of the flow coming from only 5% of the pore volume" indicates a few fast flow paths). Such a description of reservoir geometry gives the operator a means of visualizing the reservoir, and is also useful in constraining any subsequent reservoir modeling. The single drawback to the method is that it does not describe the spatial distribution of flow and storage.

If we were able to see individual fractures and fracture networks, constructing a flow-storage curve would be relatively straightforward. Flow capacity of any given fracture is proportional to the volume of fluid it carries and the fracture length itself. Darcy's law for single phase, steady state flow in a single fracture *i* is (see Nomenclature for definition of terms):

$$q_i = -\frac{k_i A_i}{\mu}\frac{\Delta P}{L_i} \tag{1}$$

The incremental flow capacity of the i^{th} fracture, assuming injection and production pressures and fluid viscosity are equal, is the ratio of that fracture's flow capacity, k_iA_i/L_i, to the total network's flow capacity.

$$f_i = \frac{k_i A_i / L_i}{\sum_{j=1,}^{\#\,frac} k_j A_j / L_j} \tag{2}$$

Incremental storage capacity follows a similar line of reasoning. The fractional storage of the i^{th} fracture is the pore volume of that fracture divided by the total fracture pore volume. It can be written as:

$$c_i = \frac{V_{pi}}{\sum_{j=1}^{\#\,frac} V_{pj}} \tag{3}$$

The Flow Capacity, F, and Storage Capacity, C, are simple summations of the individual fracture f_i and c_i. We first rearrange the individual fractures in decreasing ratios of f_i/c_i and calculate F and C as

$$F_i = F_{i-1} + f_i \tag{4}$$

$$C_i = C_{i-1} + c_i \qquad \text{for i = 1, \# frac} \tag{5}$$

Note that because the individual fracture flow and storage properties are normalized by total network properties, both F and C vary between 0 and 1.

Typically, a diagram known as an F-C diagram is constructed from the calculations discussed above. An example of such a diagram is given in Figure 1, with two example curves. The first curve in the figure is that of a uniform fracture network made up of four

fractures. Because the flow and storage is uniform in each fracture, the F-C curve is a straight line; each fracture has 25% of the flow and 25% of the storage. The 2nd curve in Figure 1 is a heterogeneous fracture network (obviously more realistic). The degree of heterogeneity is observed in the degree of departure from the uniform case. In this case, some 70% of the flow is from 20% of the fracture network pore volume, a clear indication of fast flow paths. Thus, fracture network geometry and degree of heterogeneity is given from the F-C diagram.

Of course, we are never able to determine the fracture properties *a priori*, otherwise geothermal reservoir management would be appreciably easier than it is. However, tracers "see" the same fracture properties inherent in a F-C diagram. Flow properties and storage volume are proportional to conservative tracer velocity and mean residence time.

Figure 1. Schematic diagram of a Flow-Storage Diagram for a 4 Fracture Network

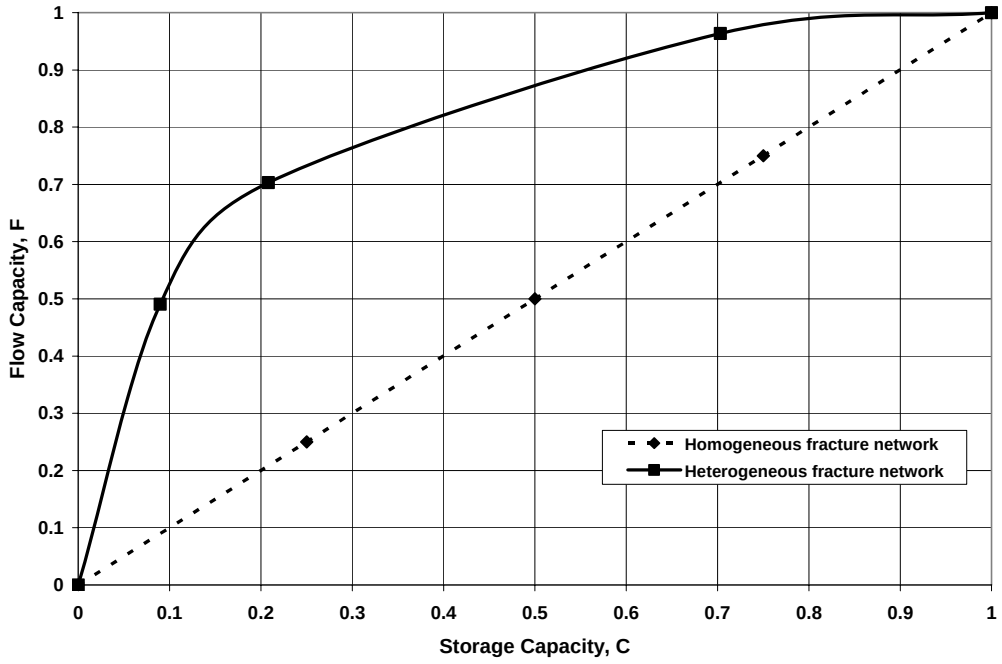

The Flow-Storage concepts may be used to estimate these properties by a suitable transformation of the tracer effluent history at any given well. The variable transformations are described below.

F-C Estimates from Tracer Tests

A conservative tracer flows with the same velocity as bulk fluid flow. The cumulative pore volume of a fracture network is proportional to the mean residence time of the tracer (e.g., Shook, 1999). How much of the tracer flows in any given fracture is likewise proportional to the flow impedance of the fracture as in Equation 2 above. Using these concepts, we can define a proxy to true F-C calculations as:

$$C(t) = \frac{\int_0^t c\tau d\tau}{\int_0^\infty ctdt} \quad (6)$$

$$F(t) = \frac{\int_0^t cd\tau}{\int_0^\infty cdt} \quad (7)$$

C(t) is simply the time-weighted reservoir volume "seen" by the tracer at time t. F(t) is the fractional cumulative amount of tracer "delivered" to the production well via the pore volume, C(t). For a given tracer effluent history, these calculations are very simple and fast on an Excel spreadsheet. The equations given above assume constant flow rates; however, variable flow rates can be handled easily as well. As an added bonus, the total pore volume follows directly from calculating C.

Example Calculations

The method described above has been tested numerically on several relatively simple, fractured geothermal reservoirs. One example is given below. The test is numerical in nature because we must have some idea of the true reservoir F-C characteristics to compare against estimates obtained from tracer tests. The reservoir is two-dimensional and rectangular, with four fractures. The background permeability and porosity are both low (k = 0.001 md; φ = 0.01). The fractures are modeled explicitly, and have varying length, permeability, porosity and mean cross sectional area, A. Fracture properties are summarized in Table 1 below.

Table 1. Summary of fracture properties for the F-C example problem.

Fracture Length	Fracture Porosity	Fracture Permeability	$\varphi_i \cdot A_i \cdot \ell_i$	$k_i \cdot A_i / \ell_i$	C_i	F_i
					0	0
170 m	0.1	650 md	17.	3.82	0.0122	0.0235
230m	0.125	1250 md	179.9	34.0	0.141	0.232
150 m	0.2	500. md	750.	83.3	0.678	0.744
360 m	.05	600 md	450.	41.7	1.	1.

Initial reservoir pressure and temperature were such that the initial fluid was single phase liquid (P = 1400 kPa; T = 175ºC).

Figure 2. Tracer history at the production well for Example 1, with closed boundaries.

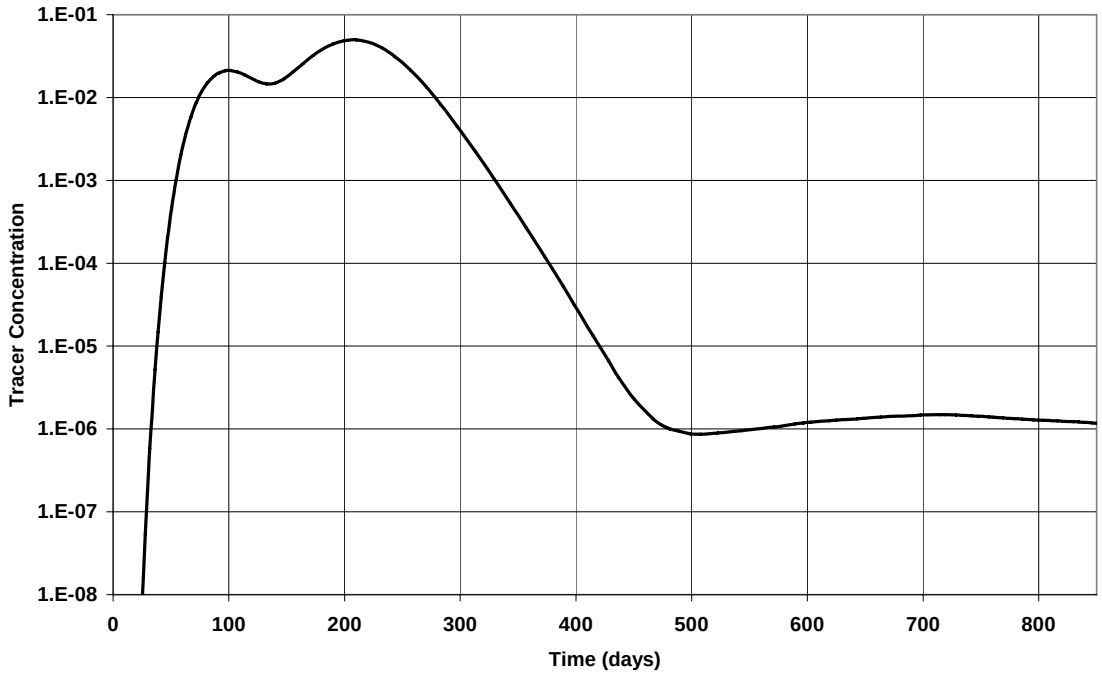

At t=0, a tracer slug was injected along with water at 35°C. The tracer was subsequently displaced by continued 35°C water injection. Production rate was constrained by a constant wellhead pressure of 900 kPa. The reservoir boundaries were closed, and a single injection and production well were used, although the issue of open boundaries is discussed below. Total simulation time for the example is 850 days.

Figure 2 shows the tracer effluent history at the production well. While we know the "true" reservoir description (e.g., 4 fractures), that information is not readily apparent in the tracer history data. A simple Excel spreadsheet application was created to calculate the F-C plot from the tracer data and Equations 6 and 7 above. The spreadsheet can be made available by the author to interested parties for interpreting other tracer tests. Results of the spreadsheet calculations are given in Figure 3, together with the correct data from Table 1 above. Also given in the figure is the estimate of the total pore volume from the spreadsheet. From Table 1 above, the pore volume estimate is off by approximately 95 m^3 (an error of about 6%). This is probably due to the very long tail in the tracer history seen in Figure 2. Corrections to account for this have been presented by Pope et al., 1994). They could have been applied here, but were not, as this was not the principle focus of the study.

Figure 3. Calculated vs. Estimated F-C properties for Example 1. Plotted symbols are from Table 1. The curve is estimated F-C from the tracer data.

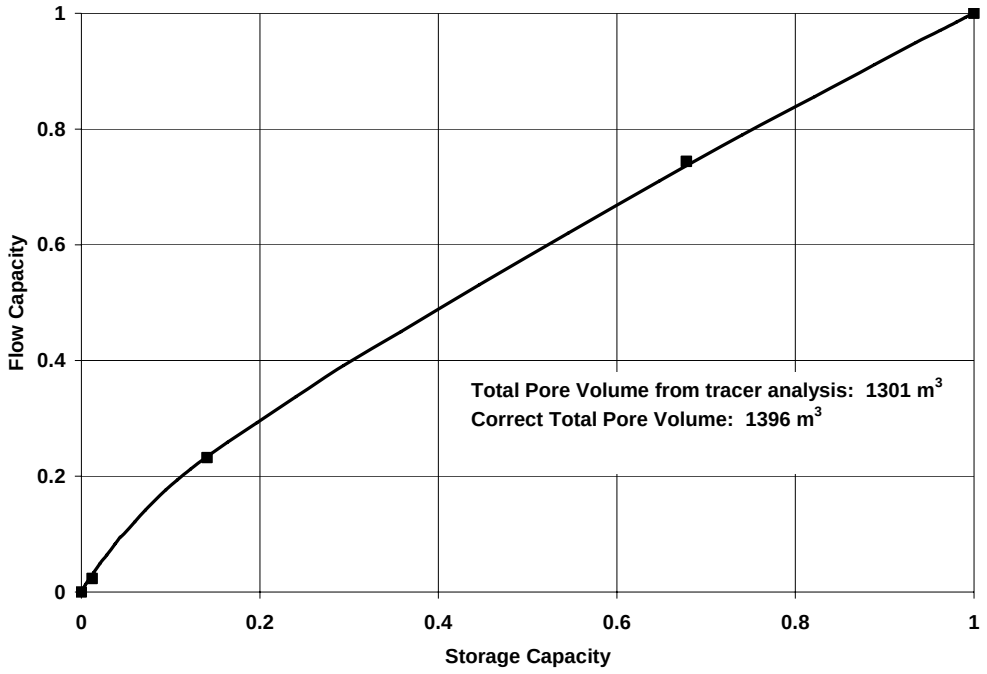

Open Boundaries

Open boundaries have no influence on the methods discussed. Tracer residence times, etc. *only* provide information on the flow network between points of injection and extraction. If reservoir boundaries are open and tracer is lost, no information is obtainable from that portion of the tracer (indeed, since the tracer is lost!). The balance of the interpretation proceeds normally, as the following example illustrates. All reservoir properties used in this simulation are as used in the closed boundary example, except the fracture geometry.

The fracture network consists of 4 fractures, with properties as given in Table 2 below. However, one fracture (# 4 in the table) is not connected to the production well; fluid in that fracture flows to a boundary and is lost. Therefore, the F-C information that could be expected from tracer test analysis cannot account for information on fracture 4. The "connected" F-C geometry (that is, excluding fracture 4) is given in Table 3.

Table 2. Summary of properties for the open boundaries example, all fractures.

Fracture Length	Fracture Porosity	Fracture Permeability	$\varphi_i \cdot A_i \cdot \ell_i$	$k_i \cdot A_i / \ell_i$	C_i	F_i
					0	0
170 m	0.1	650 md	425.	95.6	0.181	0.268
230 m	0.125	1250 md	719.	136.	0.488	0.649
150 m	0.2	500. md	750.	83.3	0.808	0.883
360 m	.05	600 md	450.	41.7	1.	1.

The tracer effluent history is given in Figure 4. Once again, the presence of 3 fractures is not especially notable from the tracer history, and only 30% of the tracer was recovered. The spreadsheet using Equations 6 and 7 was used to transform the tracer data into F-C data. The results of the transformation are given in Figure 5. Once again, excellent agreement between "correct" data (from Table 3) and the tracer interpretation is achieved. What information regarding flow and storage geometry in the interconnected fractures is preserved in the tracer data. Fracture network pore volume in this case is estimated as 1606 m^3 (Figure 5), an error of about 19 m^3 (1.1%).

Figure 4. Tracer history for Example 2, open boundaries.

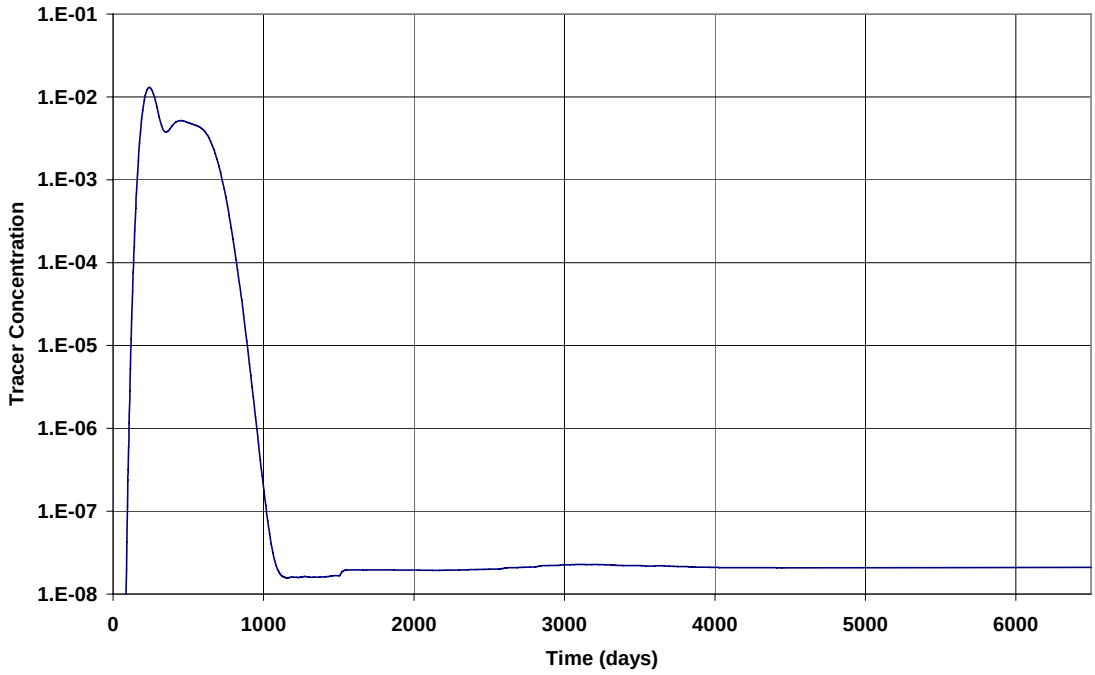

Figure 5. Comparison in interconnected F-C properties and those estimated from tracer data for the open boundary example.

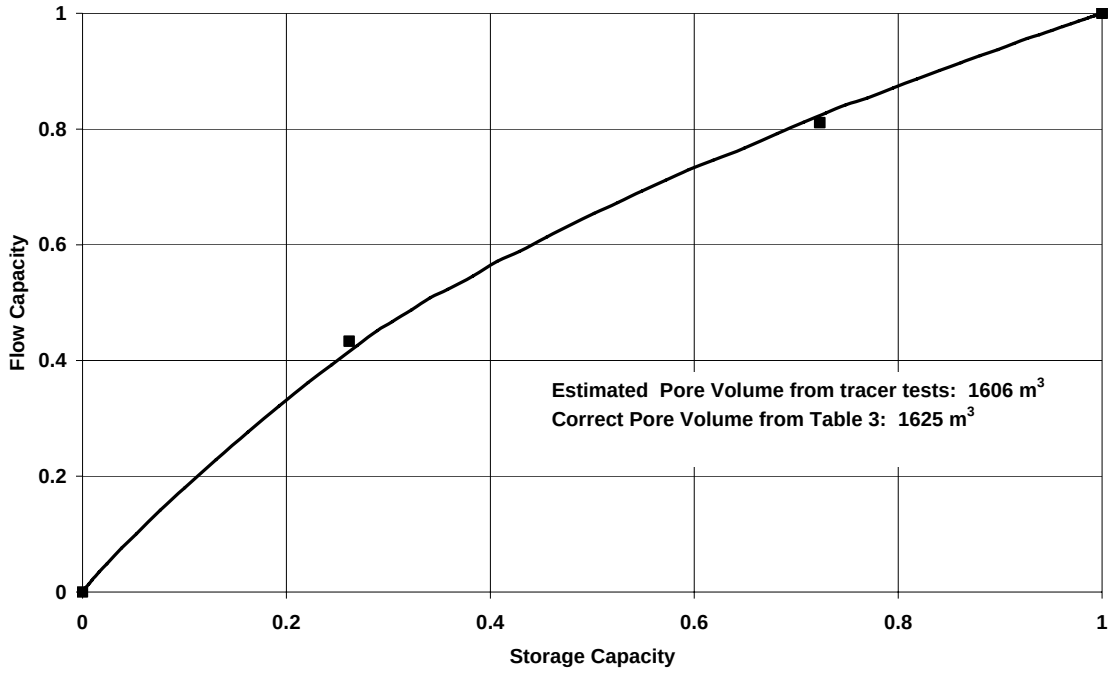

Table 3. Summary of properties for the F-C example problem, interconnected fractures only.

Fracture Length	Fracture Porosity	Fracture Permeability	$\varphi_i \cdot A_i \cdot \ell_i$	$k_i \cdot A_i / \ell_i$	C	F_i
					0	0
170 m	0.1	650 md	425.	95.6	0.262	0.433
150m	0..5	500. md	750.	83.3	0.723	0.811
360 m	0.05	600. md	450.	41.7	1.	1.

Summary and Future Work

A method for determining relative flow and storage capacity for fractured, geothermal reservoirs is presented. The method transforms tracer effluent data into data useful in plotting F-C diagrams. Such diagrams can be used semi-quantitatively: "x% of flow comes from y% of pore volume." The single drawback to the method is that no information regarding the spatial distribution of the fracture network is preserved. The method works equally well in open or closed reservoirs. The method provides a good description of the fracture network connecting injection and extraction points.

Embedded in the definition of flow capacity and storage capacity is the fracture area, A_i. Given independent estimates of fracture (or rubble zone) length and porosity, we can estimate an average fracture area. This may allow the estimation of specific surface area for heat transfer. This continues to be an area of active research at INEEL.

We are most interested in applying this technique to real tracer tests in geothermal fields, and solicit the interest and collaboration of any operator similarly interested.

Acknowledgements
This work was supported by the U.S. Department of Energy, Assistant Secretary for Energy Efficiency and Renewable Energy, under DOE Idaho Operations Office Contract DE-AC07-99ID13727.The author gratefully acknowledges a careful review of the manuscript by J.L. Renner.

Nomenclature

A_i	mean cross-section area of the i^{th} fracture (pore volume divided by length) [=] L^2
c	Tracer concentration at a production well [=] dimensionless
C(t)	Tracer test-inferred cumulative storage capacity [=] dimensionless
c_i	Incremental storage capacity of the i^{th} fracture [=] dimensionless
C_i	Cumulative storage capacity function of the fracture network [=] dimensionless
F(t)	Tracer test-inferred cumulative flow capacity [=] dimensionless
f_i	Incremental flow capacity of the i^{th} fracture [=] dimensionless
F_i	Cumulative flow capacity function of the fracture network [=] dimensionless
k_i	permeability of the i^{th} fracture [=] L^2
L_i	length of the i^{th} fracture [=] L
q_i	volumetric fluid flow in i^{th} fracture [=] L^3/t
t	time
V_{pi}	pore volume of the i^{th} fracture [=] L^3
ΔP	pressure difference between injection and production well [=] kPa
μ	fluid viscosity [=] kPa-s

References

Adams, M.C., J.J. Beall, S.L. Enedy, P.N. Hirtz, P.Kilbourn, B.A. Koenig, R.Kunzman and J.L. Smith, 2001, "Hydrofluorocarbons as geothermal vapor-phase tracers," *Geothermics*, 30(6), pp 747-775.

Axelsson, G., O.G. Flovenz, S. Hauksdottir, A. Hjartarson, and J. Liu, 2001, "Analysis of tracer test data, and injection-induced cooling, in the Laugaland geothermal field, N-Iceland," *Geothermics*, 30(6), pp 573-589.

Gunderson, R., M. Parini, and L. Sirad-Azwar, 2002, "Fluorescein and Napthalene Sulfonate Liquid Tracer Results at the Awibengkok Goethermal Field, West Java, Indonesia," *Proc.* 27th Workshop on Geothermal Reservoir Engineering, Stanford, Ca.

Matsunaga, I., N. Yanagisawa, H. Sugita, and H. Tao, 2002, "Reservoir Monitoring by Tracer Testing During a Long Term Circulation Test at The Hijiori HDR Site," ," *Proc.* 27th Workshop on Geothermal Reservoir Engineering, Stanford, Ca.

Pope, G.A., M. Jin, V. Dwarakanath, B.A. Rouse, K. Sepehrnoori, 1994, "Partitioning Tracer Tests to Characterize Organic Contaminants," Proc., 2nd Tracer Workshop, U.

Texas, Austin, edited by T. Bjornstad and G. Pope, Institute for Energy Technology, N-2007, Kjeller, Norway, pp. 65- 71.

Robinson, B. A. and J.W. Tester, 1984, "Dispersed Fluid Flow in Fractured Reservoirs: An Analysis of Tracer-Determined Residence Time Distributions," J. Geophysical Research, 89(B12), pp 10374-10384.

Rose, P.E., Apperson, K.D., and Faulder, D.D.: "Fluid Volume and Flow Constraints for a Hydrothermal System at Beowawe, Nevada," SPE Paper 38762, presented at the 1997 Annual Technical Conference of the SPE, Oct. 5-8, 1997, San Antonio.

Rose, P.E., W.R. Benoit, and P.M. Kilbourn, 2001, "The Application of the Polyaromatic Sulfonates as Tracers in Geothermal Reservoirs," *Geothermics*, 30(6), pp 617-640.

Shook, G.M., 2001, "Predicting thermal breakthrough in heterogeneous media from tracer tests," *Geothermics*, 30(6), pp 573-589.